ORIGINAL ARTICLE   **Open Access**

Thymine/adenine diblock-oligonucleotide monolayers and hybrid brushes on gold: a spectroscopic study

Caitlin Howell[1,2,3*], Hicham Hamoudi[2,4] and Michael Zharnikov[2*]

Abstract

Background: The establishment of spectroscopic analysis techniques for complex, surface-bound biological systems is an important step toward the further application of these powerful experimental tools to new questions in biology and medicine.

Methods: We use a combination of the complementary spectroscopic techniques of X-ray photoelectron spectroscopy, Infrared reflection-absorption spectroscopy, and near-edge x-ray absorption fine structure spectroscopy to monitor the composition and molecular orientation in adenine/thymine diblock oligonucleotide films and their hybridized brushes on gold.

Results: We demonstrate that the surface-bound probe molecules, consisting of a binding adenine block, d(A), and a sensing thymine block, d(T), deviate from the ideal L-shape model due to the internal intra- and intermolecular hybridization. This effect becomes more pronounced with increasing length of the d(A) block. Nevertheless, these films were found to hybridize well with the complementary target d(A) strands, especially if they were treated in advance to reduce internal interaction between the molecules. In spite of the structural complexity of these films, the hybridization efficiency correlated well with the potential accessibility of the sensing d(T) blocks, defined by their lateral spacing.

Conclusions: These findings are a good demonstration of the strength of multi-technique spectroscopic analysis when applied to assemblies of biological molecules intrinsically prone to complex interactions.

Keywords: ssDNA film, Diblock-oligonucleotide, HRXPS, NEXAFS, IRRAS

Background

Understanding the properties of and processes involving biological molecules on surfaces and interfaces is at the heart of many critical issues in biology and medicine [1-3]. The organization and hybridization of surface-bound DNA in particular is an important component in many established, new, and emerging medical and other biology-based technologies, including microarrays [3-5], DNA-decorated nanoparticles [6,7], and DNA computing [8,9]. In systems such as these, the tethering of the DNA strands to a solid surface is necessary for greater control over density, orientation, and hybridization processes. Nevertheless, precise measurement or reconstruction of these parameters and processes through conventional means such as microscopy and fluorescent labeling [10] or surface plasmon resonance (SPR) spectroscopy [11,12] can be challenging due to the nanoscale nature of the DNA molecules involved as well as the non-specific character of these techniques.

Different types of spectroscopy have been shown to be useful for such nanoscale analysis, as they inherently give specific, label-free, and molecular-level information. Techniques such as X-ray photoelectron spectroscopy (XPS) [13,14], near-edge X-ray absorption fine structure (NEXAFS) spectroscopy [15-18], time-of-flight secondary ion mass spectrometry (ToF-SIMS) [19-21],

* Correspondence: chowell@seas.harvard.edu; Michael.Zharnikov@urz.uni-heidelberg.de
[1]Institute of Toxicology and Genetics, Karlsruhe Institute of Technology, Hermann-von-Helmholtz-Platz 1, 76344, Eggenstein-Leopoldshafen, Germany
[2]Applied Physical Chemistry, University of Heidelberg, Im Neuenheimer Feld 253, 69120, Heidelberg, Germany
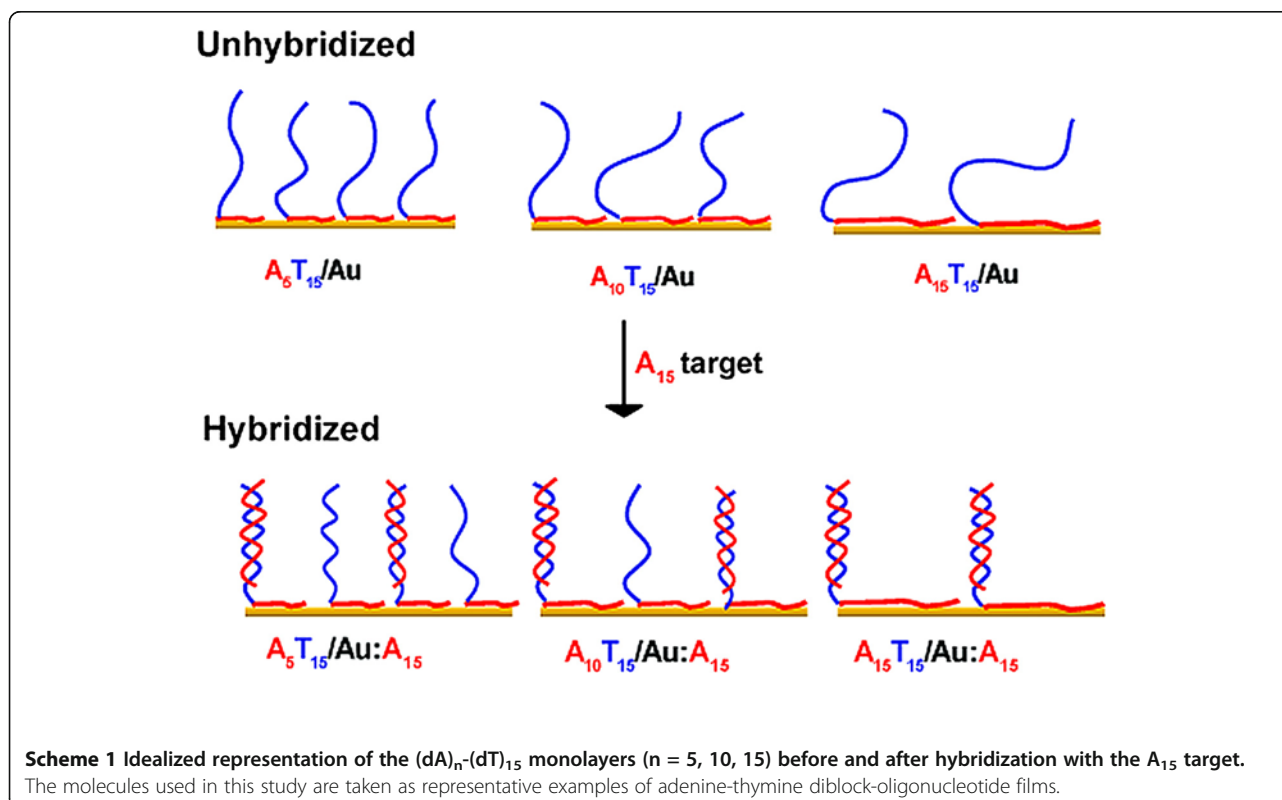Full list of author information is available at the end of the article

sum-frequency-generation (SFG) spectroscopy [22,23], and infrared reflection-absorption spectroscopy (IRRAS) [24,25] can be used to determine composition, content, molecular orientation and hybridization behavior of DNA assemblies. Yet despite the large amounts of potential information obtainable through use of these methods, the interpretation of spectra from biological samples, including surface-bound DNA, can be difficult, often resulting in the restriction of the use of these techniques to simplified or relatively straightforward systems. In order to expand the use of spectroscopic methods, comparative studies on biological molecules capable of acting in increasingly complex ways are needed.

In this context, Opdahl and co-workers [24] recently reported a method of controlling the grafting density in films of single-stranded DNA (ssDNA) on gold substrates by exploiting the fact that adenine nucleotides have a higher affinity for gold than thymine nucleotides. They created films in which DNA molecules consisting of a block of adenine nucleotides connected to a block of thymine nucleotides adsorbed in a (presumably) L-shaped configuration on a gold surface. In an ideal version of this system, illustrated in Scheme 1, the d(A) block serves as the binding unit which can be shortened or lengthened to increase or decrease the density, respectively. The remaining d(T) block, either acting as or connected to the sensing portion of the molecule, is free to protrude into ambient, associate with the surface-bound d(A) block, or hybridize with a complimentary target [11,12]. In reality, a systematic lengthening of the d(A) block also brings increasing complexity to the system, changing the layer from being relatively tightly-packed and well-defined to one in which more space exists between the protruding d(T) blocks. This allows both more freedom of movement and a greater probability of the formation of stable inter- or intra-molecular hybrids between the complimentary d(A) and d(T) portions of the molecules. Such systematic changes may affect the number and quality of any hybrids that are then formed by introduction of a complimentary target strand, perhaps the most important consideration in the application of these molecules to biotechnology and medicine.

Here, we use the abovementioned diblock-oligonucleotides to systematically increase the degree of complexity in DNA hybrid brushes. Using a combination of high-resolution XPS, IRRAS, and NEXAFS spectroscopy to gather complimentary information on molecular density, content, and orientation, we present a molecular-level picture of the effects of increasing complexity on these parameters. We find that as the DNA hybrid systems become capable of more complex interactions the predictability of orientation becomes increasingly difficult, even as the molecular content continues to change as expected. These results highlight the importance of using multiple spectroscopic techniques to gain a complete picture of

Scheme 1 Idealized representation of the (dA)$_n$-(dT)$_{15}$ monolayers (n = 5, 10, 15) before and after hybridization with the A$_{15}$ target. The molecules used in this study are taken as representative examples of adenine-thymine diblock-oligonucleotide films.

parameters of and processes involving biological systems on the molecular scale, especially as the level of complexity increases.

Methods
Materials
Gold substrates were produced by using radio frequency magnetron sputtering to coat silicon wafers (Si-Mat Silicon Materials, Kaufering, Germany) with a chromium adhesion later, followed by a gold layer. The result was a 100 nm-thick polycrystalline gold film with a predominant (111) orientation. The coated wafers were cut into appropriate sizes, cleaned by exposure to UV/ozone (UV cleaner 42–220, Jelight) for 2.5 hrs, and rinsed thoroughly with HPLC-grade water immediately prior to film deposition.

High performance liquid chromatography-purified DNA sequences were purchased from Sigma–Genosys (Steinheim, Germany): 5'-$(dA)_5$-$(dT)_{15}$-3', 5'-$(dA)_{10}$-$(dT)_{15}$-3', 5'-$(dA)_{15}$-$(dT)_{15}$-3', probe sequences, as well as a complimentary $(dA)_{15}$ target. These will be referred to hereafter as A_5T_{15}, $A_{10}T_{15}$, $A_{15}T_{15}$, and A_{15}, respectively (see Scheme 1). Block-DNA containing only adenine and thymine was chosen over block-DNA containing a random sequence of all four nucleobase types in order to facilitate interpretation of the spectra. The Tris–HCl, EDTA, and NaCl used in the deposition and hybridization buffers were obtained from Sigma-Aldrich (Seelze, Germany).

DNA Immobilization and hybridization
DNA brushes were formed by incubating gold wafers for 40 h at 37°C in 1 M $CaCl_2$–TE buffer (10 mM Tris–HCl and 1 mM EDTA, pH=7.08) containing a 3 μM DNA solution. After incubation, unhybridized samples were rinsed for 1 min under flowing deionized water (resistivity >18.2 MΩ cm) to remove excess DNA and dried with N_2 [13].

Samples intended for hybridization were rinsed for either one full minute under deionized water or for 30 seconds under deionized water, followed by 30 seconds under flowing 0.1 M NaOH, followed again by 30 seconds under deionized water. The NaOH rinse was added in an effort to destabilize any partial inter-molecular hybrids and improve overall hybridization and orientation [12]. After rinsing, these samples were placed in a 1M NaCl buffer containing 3 μM of the $(dA)_{15}$ target sequence for 7 h at room temperature. Following incubation, samples were rinsed with 1 M NaCl buffer for 1 min, briefly dipped in deionized water to remove excess salts [26], and finally dried under flowing N_2 according to previously described procedures [11]. It should be noted that exposing surface-bound DNA hybrids to pure water, while necessary to prepare them for HRXPS and NEXAFS spectroscopy

measurements, is known to affect their stability [11,26]. However, a recent systematic study on the subject has shown that when the samples are rinsed with small volumes of water (~0.5 mL), such as those used here, breakup of such hybrids is minimal [26].

High Resolution X-ray Photoelectron Spectroscopy
HRXPS measurements were performed at the HE-SGM beamline of the synchrotron storage ring BESSY II in Berlin, Germany. The measurements were conducted under UHV conditions at a base pressure better than 1.5×10^{-9} mbar and at room temperature. The spectral acquisition time was selected such that no noticeable damage by the primary X-rays occurred during the measurements [27-30]. The acquisition of the spectra was carried out in normal emission geometry with an energy resolution of ~0.4 eV. The energy scale was referenced to the Au $4f_{7/2}$ peak at 83.95 eV [31].

The spectra were fitted with symmetric Voigt functions and either a Shirley or linear background. The fits were carried out self-consistently, i.e. the same peak parameters were used for identical spectral regions. The film thickness was determined on the basis of the intensity ratios of the C 1s and Au 4f emissions [32], assuming a standard exponential attenuation of the photoelectron signal and using the attenuation lengths reported by Lamont and Wilkes [33].

The thickness was then used to calculate the density of the surface-adsorbed DNA molecules in the A_5T_{15}/Au film according to the procedures developed by Petrovykh et al. [13,14]. Due to minor carbon contamination in the $A_{10}T_{15}$/Au sample, the density values for this and the $A_{15}T_{15}$/Au films were calculated on the basis of the averaged intensity of the characteristic N 1s, P 2p, and O 1s signals and corrected for molecular composition. Density values of 1.40×10^{13}, 1.02×10^{13}, and 8.96×10^{12} molecules cm^{-2} were obtained using this method for the A_5T_{15}/Au, $A_{10}T_{15}$/Au, and $A_{15}T_{15}$/Au films, respectively. These values are comparable to those reported for similar films [24], although somewhat lower. This is most likely due to the fact that the C1s/Au4f intensity ratio was used to calculate thickness rather than the intensity of the Au 4f emission from sputter-cleaned gold [13,14].

Infrared reflection-adsorption spectroscopy
IRRAS was performed on a Vertex 80 Infrared spectrometer (Bruker Optics, Ettlingen, Germany) using an A518 IRRAS sampling stage with an 80° fixed-angle gracing incidence. The signal was recorded by a D313 narrow-band MCT detector cooled by liquid N_2. A gold substrate covered with a perdeuterated dodecanethiol self-assembled monolayer was used as a reference. Background measurements were performed with 1024 scans, and suppression of the water signal in samples was
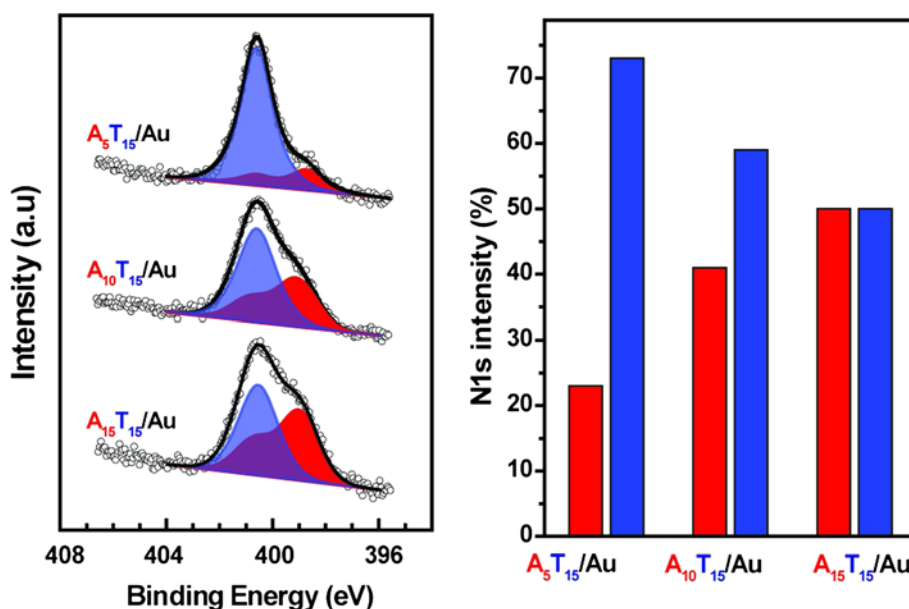
Figure 1 Left: N 1s HRXPS spectra of unhybridized DNA brushes. The spectra are decomposed into the components assigned to thymine (blue) and adenine (red). Right: Relative intensities of the adenine (red) and thymine (blue) components.

usually achieved between 1000 and 3000 scans. Baseline correction and data evaluation were performed using the Opus 6.5 IR software package (Bruker Optics).

Near-edge X-ray absorption fine structure spectroscopy

NEXAFS and HRXPS spectra were collected at the same beamline. The acquisition of the NEXAFS spectra was performed at the C, N, and O K-edges in the partial electron yield (PEY) mode with retarding voltages of −150, −300, and −350 V, respectively. Linear polarized synchrotron light with a polarization factor of ~0.91 was used. The energy resolution of the whole setup was estimated to be on the order of ~0.3 eV, slightly dependent on the photon energy. To monitor the orientational order in the films, the incidence angle of the light was varied from 90° (*E*-vector in the surface plane) to 20° (*E*- vector near the surface normal) in steps of 10-20° (the angles are defined with respect to the surface plane) [34]. This approach is based on the dependence of the cross-section of the resonant photoexcitation process on the orientation of the electric field vector of the synchrotron light with respect to the molecular orbital of interest (so-called linear dichroism in X-ray absorption) [34]. This effect results in a characteristic dependence of an adsorption resonance intensity on the incidence angle of X-rays, as long as there is some orientational order present in the probed system. The photon energy (PE) scale was referenced to the pronounced π* resonance of highly oriented pyrolytic graphite at 285.38 eV [35].
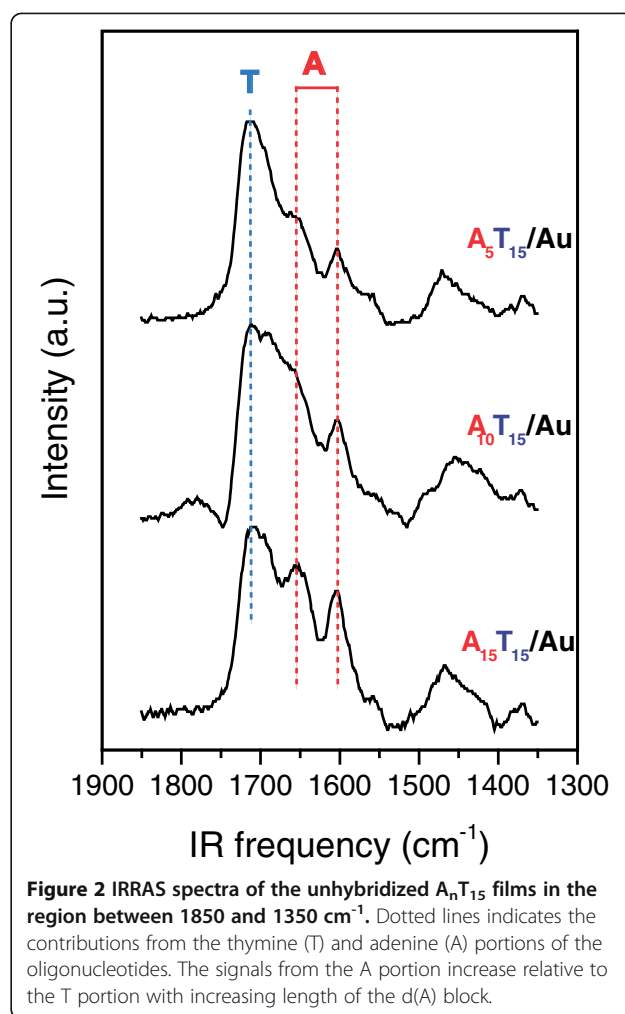
Results and discussion
Unhybridized DNA brushes

Unhybridized films were examined to verify the quality of the deposited DNA layers and to gather an initial picture of the system before the formation of hybrids. Figure 1 (left) shows the N 1s HRXPS spectra of the initial unhybridized A_5T_{15}, $A_{10}T_{15}$, and $A_{15}T_{15}$ films. All three spectra have been decomposed into the components associated with thymine and adenine, with thymine appearing as a single peak with a binding energy of ~400.5 eV and adenine as a doublet with individual peaks at ~398.7 and ~400.5 eV and an intensity ratio of 2:1 [11,18,24]. The expected increase in the adenine content with increasing length of the d(A) block can be clearly seen, in agreement with previous reports on similar films [11,24]. The relative intensities of the thymine and adenine signals are presented in Figure 1 (right). These parameters exhibit the expected trend with the increasing length of the d(A) block but, after normalization to the number of nitrogen atoms present in thymine (2) and adenine (5), give a much higher proportion of thymine than can expected from the molecular composition alone. This seeming disagreement can be explained by the stronger attenuation of the photoelectron signal from the d(A) block serving as the molecular anchor and located, partly or almost completely, underneath the d(T) block. Note that the attenuation is especially strong at the kinetic energy of the N 1s photoelectrons (~180 eV; an attenuation length of 0.84 nm [33]), which explains why this effect was less

pronounced in previous work relying on laboratory XPS systems [13,24,25] which have much higher excitation energy and, subsequently, higher photoelectron kinetic energies. Note also that the respective attenuation factor (~2.5) does not change significantly with the increasing length of the d(A) block, which contradicts the idea of the L-shape adsorption model and suggests that the exact adsorption geometry of the A_nT_{15} molecules depends on the molecular composition. Nevertheless, the presence of such a strong attenuation supports the general view of the d(A) and d(T) blocks in the A_nT_{15} films as binding and sensing units, respectively.

In Figure 2, the IRRAS spectra of the A_nT_{15} films in the region from 1850 to 1350 cm^{-1} are displayed. All three films show a strong peak at ~1710 cm^{-1}. This peak has been attributed to stretching vibrations of the C=O bond in the thymine nucleotides which are not in direct contact with gold [15], and indicates that the d(T) portions of the DNA molecules were indeed extending into the ambient as predicted, rather than associating with the substrate. The spectra also display features typical of adenine nucleobases [36], with a peak at ~1650 cm^{-1}, which has previously been assigned to NH_2 bending modes, and another at ~1600 cm^{-1}, assigned to NH_2 bending modes or their combination with C=N stretching modes [25]. With the increasing length of the d(A) block, the corresponding adenine features increase in intensity relative to the thymine features. This is in agreement with the HRXPS results as well as with IRRAS results on similar samples presented in previous studies [24].

NEXAFS spectroscopy provides information on the chemical composition of a film by sampling the electronic structure of the unoccupied molecular orbitals, as well as on the orientational order of the adsorbed molecules through examination of the angular dependence of the resonant excitations [34]. The chemical composition is usually probed by collecting spectra at the so-called magic angle of X-ray incidence (55˚). These spectra are not affected by orientational effects and are therefore solely representative of the film composition. Such spectra of the A_nT_{15} films collected at the N K-edge are shown in left-hand panel of Figure 3. The spectra of all films exhibit a superposition of two characteristic resonances of thymine at 401.1 eV (corresponding to the N 1s →LUMO transition) and 402.0 eV (corresponding to the N1s →LUMO+1 transition), and two resonances from adenine at 399.4 eV (N 1s →LUMO transition) and 401.3 eV (N 1s →LUMO + 2 transition) [37]. The resonances of thymine are merged, with the one at 401.1 eV being more intense, while the resonances of adenine are well separated, with the 399.4 eV peak being much more intense than the one at 401.3 eV [37]. Accordingly, only a slightly asymmetric resonance of thymine at 401.1

Figure 2 IRRAS spectra of the unhybridized A_nT_{15} films in the region between 1850 and 1350 cm^{-1}. Dotted lines indicates the contributions from the thymine (T) and adenine (A) portions of the oligonucleotides. The signals from the A portion increase relative to the T portion with increasing length of the d(A) block.

eV (marked by blue) and a sharp resonance of adenine at 399.4 eV (marked by red) are clearly present in the spectra of the A_nT_{15} films in Figure 3 (left). Since the overlap between these resonances is negligible, it is possible to identify unique adenine and thymine contributions in the spectra. As seen in Figure 3, the relative intensity of the adenine contribution increases with the increasing length of the d(A) block while that of thymine decreases, in agreement with the expected film composition and the HRXPS results.

Beyond the chemical composition, information on average molecular orientation can be obtained from NEXAFS data by considering the angular dependence of the resonance intensity [34]. A suitable way to monitor such dependence is to plot the spectra acquired at the normal and gracing incidence angles of the X-ray beam. The orientational order present in the probed system will then manifest itself as difference peaks at the positions of the characteristic absorption resonances. The sign and intensity of these peaks will then provide
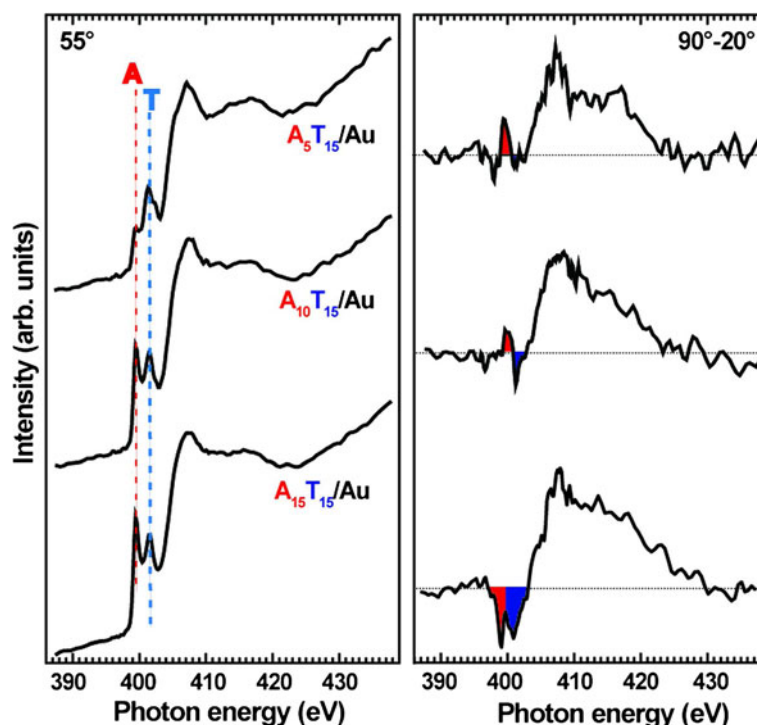
Figure 3 N K-edge NEXAFS spectra of the unhybridized A_nT_{15} films. Left: Spectra acquired at an X-ray incidence angle of 55°. The positions of the most pronounced, π*-like absorption resonances of thymine (T) and adenine (A) are marked by the thin vertical blue (T) and red (A) dotted lines. Right: Difference of the spectra acquired at X-ray incidence angles of 90° and 20°. Adenine and thymine contributions are indicated by the red or blue fill (respectively), with an upward or downward orientation indicating a mostly horizontal or vertical orientation (respectively) of the nucleotides relative to the surface. Horizontal dashed lines correspond to zero for the individual difference spectra.

information on the exact molecular geometry and degree of the orientational order. To this end, the difference spectra of the A_nT_{15} films and derived brushes of DNA hybrids were considered in detail.

Generally, the nucleobases are assumed to be oriented perpendicularly to the ssDNA backbone, even though they possess some flexibility in orientation due to rotation relative to the backbone and from irregular bends in the backbone. But even taking into account this flexibility, a very strong positive peak would arise in the difference NEXAFS spectra from a film in which the DNA strands are parallel to the surface (nucleobases would then be predominantly oriented perpendicular to the substrate), and a very strong negative peak would be seen when all DNA molecules are oriented perpendicular to the surface (the nucleobases would then be predominantly oriented parallel to the substrate) [15,17,38]. In the case of ideal L-shape diblock-oligonucleotides [24,36], we would therefore expect to see a very strong positive peak from the parallel surface-binding adenine block and a very strong negative peak from the perpendicular sensing thymine block. In the case of deviations from the ideal parallel or perpendicular alignment, as presumably occurs in a real diblock-oligonucleotide system [15], we would expect to see less intense (but still

clearly visible) positive adenine peaks and negative thymine peaks. In the ultimate case of partial or complete disordering of either the d(A) or d(T) blocks, no respective difference peaks would be perceptible.

The right-hand panel of Figure 3 shows the difference between the spectra of the A_nT_{15} films collected at 90° and 20°. The A_5T_{15} film shows a strong positive adenine peak and a very weak negative thymine peak indicating, as expected, a predominantly parallel-to-the-substrate alignment of the adenine blocks of the DNA strands. Unexpectedly, however, this also indicates a near lack of any sort of orientational order in the thymine blocks. The most probable reason for this behavior is the interaction of the d(T) blocks with the surface-bound d(A) nucleotides [12], which can be explained by partial intra-molecular and intermolecular hybridization. These hybrids could have formed either in solution prior to deposition, or after contact with the substrate. More sophisticated explanations are possible as well, including complex hybridization scenarios involving several molecules [26,39,40]. However, which of these configurations is dominant is not something that can be directly determined via NEXAFS spectroscopy but, presumably, requires its combination with theoretical calculation of most energetically favorable structural motifs.

The $A_{10}T_{15}$ film, in contrast, shows a predominantly perpendicular alignment of the thymine block as well as a predominantly parallel orientation of the adenine block. However, the intensities of the difference peaks are small, indicating that the extent of nucleobase alignment is small as well. As the $A_{10}T_{15}$ molecules have the potential to form twice the number of base pairs compared to the A_5T_{15} molecules, it would be expected that any intermolecular hybrids formed in solution prior to deposition would be more stable. This may be one explanation for the results seen here, as a greater number of intermolecular hybrids would result in a smaller overall parallel ordering of the adenine nucleotides due to the presence of d(A) blocks with perpendicular orientation. In turn, the greater stability of these remaining inter- and intramolecular hybrids, compared to those of the A_5T_{15} molecules, would result in a more stable perpendicular order in the thymine nucleotides [23]. However, the still relatively low maximum number of base pairs overall would likely mean that these types of intermolecular hybrids are not very stable [41,42] and thus unlikely to be the most common species in the $A_{10}T_{15}/$ Au film. This would explain the continued dominance of the parallel orientation in the adenine nucleotides in this sample seen in the NEXAFS data. Note that the molecular orientations implied by the 90°–20° difference spectra in Figure 3 for the A_5T_{15}/Au and $A_{10}T_{15}/Au$ films are in full agreement with previous NEXAFS results [18].

The d(A) and d(T) blocks of the $A_{15}T_{15}$ molecules, in contrast to the A_5T_{15} and $A_{10}T_{15}$ species, are fully complimentary in length, which should create the most stable inter- and intramolecular hybrids in solution. The most stable configuration of these molecules should be the full 30-base pair double helix formed from aligning two $A_{15}T_{15}$ strands. Upon exposure to the gold surface and subsequent rinsing and drying, the NEXAFS data reveal that both the adenine and thymine portions of these molecules are preferentially oriented perpendicular to the surface, suggesting that a large portion of the thymine blocks and at least a part of the adenine blocks are remaining upright. One molecular configuration which would be consistent with these data would be the attachment of the DNA molecules in complete hybrid form via only a portion of the d(A) block. Other arrangements could also exist, including an L-shaped configuration in which a second molecule is hybridized only with the d(T) portion, however the intensity of the adenine peak in the NEXAFS 90°–20° data suggests that on average in this film more d(A) blocks are oriented upright than lying flat, in clear contrast to the A_5T_{15}/Au and $A_{10}T_{15}/$ Au layers.

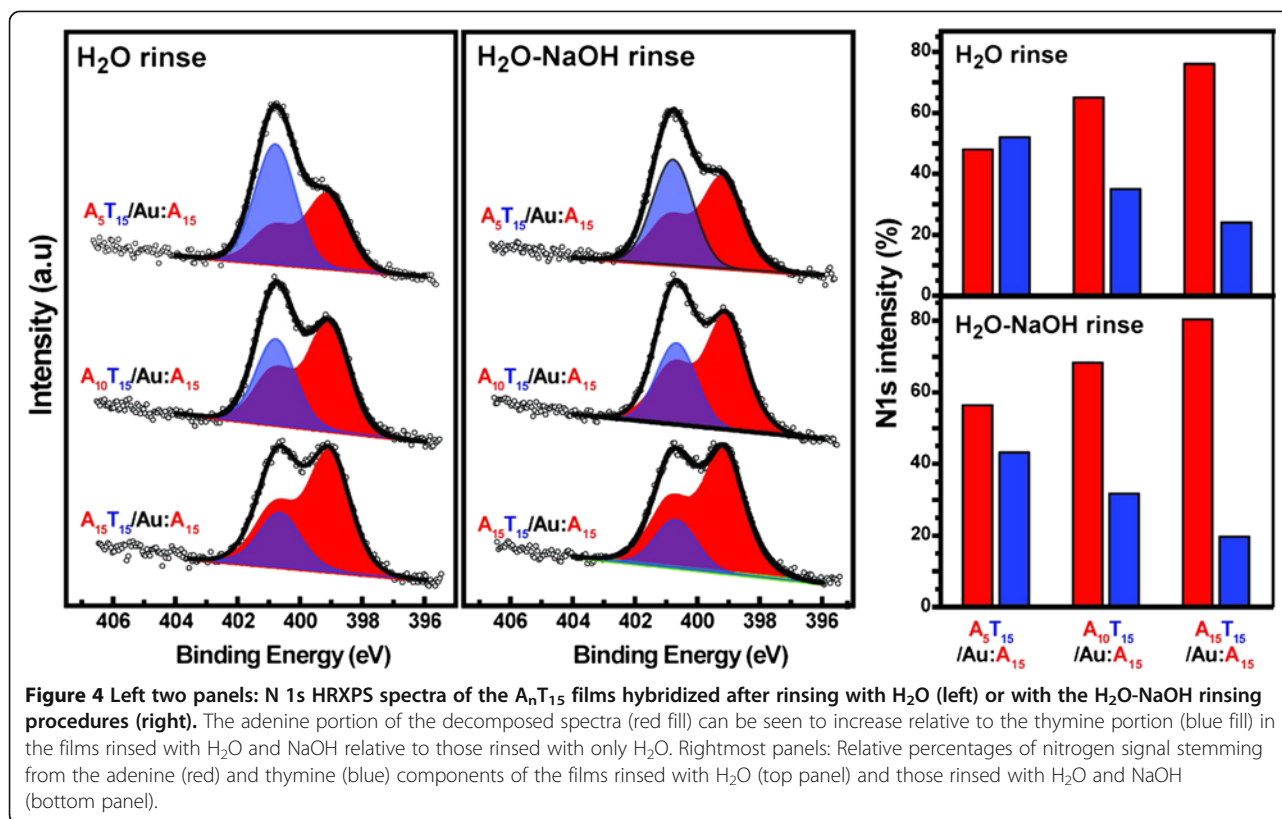Summarizing, the HRXPS, IRRAS, and NEXAFS composition data give expected results for the unhybridized A_nT_{15} films, confirming their quality and composition compared to previously tested films of this type [24]. The NEXAFS results presented here support the theory of complex hybridization interactions affecting these layers, as the simplest molecular arrangements necessary to produce the observed spectra become more complex from the A_5T_{15}/Au, to $A_{10}T_{15}/Au$, to the $A_{15}T_{15}/Au$ film.

DNA hybrid brushes

Hybridization was performed using two approaches: first, by rinsing the initial unhybridized films with only pure water, and second, by rinsing the films with water, followed by a 0.1 M solution of NaOH, then water a final time. The latter approach was intended to further destabilize any inter- or intra-molecular hybrids in the probe film with the aim of improving both the number and quality of the hybrids formed upon exposure to the complimentary A_{15} target [11].

Figure 4 shows the HRXPS data for the resulting brushes of DNA hybrids, with the two left-hand panels displaying the N 1s spectra, and the vertically arranged right-hand panels presenting the relative intensities of the adenine and thymine signals for each particular spectrum. The intensity of the adenine signal is clearly higher in these spectra as compared to the unhybridized A_nT_{15} films (Figure 1, right panel), as expected due to the presence of the A_{15} target. A comparison between the intensity values for the films rinsed with alternating H_2O and NaOH to those rinsed with only H_2O shows that the addition of NaOH increases the amount of adenine in all cases, also as predicted.

Beyond this qualitative conclusion, it is possible to perform a numerical analysis of the intensity values in Figure 4 to get at least a coarse estimate of the degree of hybridization. Normalizing the intensities to the number of nitrogen atoms in adenine (5) and thymine (2) and assuming the same attenuation of the photoemission signal for the d(A) anchor of the A_nT_{15} probe species (a factor of 2.5; see above), we obtained the following values for the extent of hybridization in the H_2O-rinsed $A_nT_{15}/Au:A_{15}$ brushes: 24%, 46%, and 87% for $n = 5$, 10, and 15, respectively. For the films rinsed with alternating H_2O and NaOH, these values were calculated to be 39%, 57%, and ~100% for $n = 5$, 10, and 15, respectively. Note that these values can be considered as coarse estimates only, since the attenuation factor for the photoemission signal from the d(A) anchor of the A_nT_{15} probe can change after the hybridization event. It is most likely that this factor would decrease as the inter- and intramolecular (probe) hybrids are disrupted and upright target-probe hybrids are formed, resulting in a partial uncovering of the d(A) anchors. Thus, the values of the hybridization efficiency calculated here are presumably the upper limits of the real values. Note also that these

Figure 4 Left two panels: N 1s HRXPS spectra of the A_nT_{15} films hybridized after rinsing with H_2O (left) or with the H_2O-NaOH rinsing procedures (right). The adenine portion of the decomposed spectra (red fill) can be seen to increase relative to the thymine portion (blue fill) in the films rinsed with H_2O and NaOH relative to those rinsed with only H_2O. Rightmost panels: Relative percentages of nitrogen signal stemming from the adenine (red) and thymine (blue) components of the films rinsed with H_2O (top panel) and those rinsed with H_2O and NaOH (bottom panel).

values represent coarse estimates only since they are based on a single sample for each particular system. However, qualitatively similar differences between the outcomes of the H_2O and H_2O-NaOH rinsing procedures were observed for all A_nT_{15} samples, which strengthens the reliability of the conclusions.
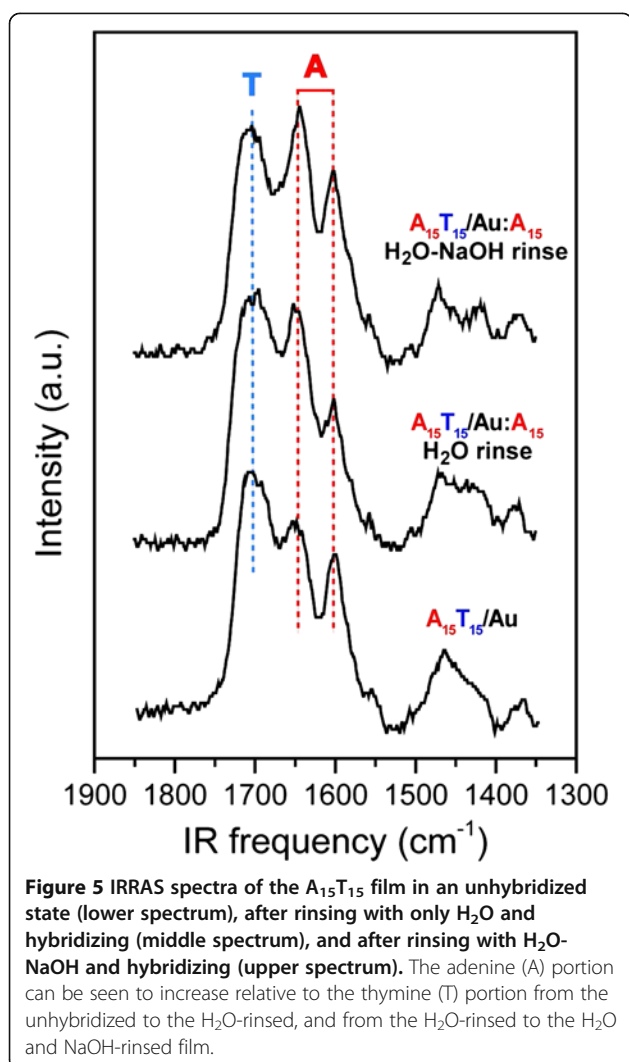
Apart from this uncertainty, two tendencies are apparent. First, the H_2O-NaOH rinsing procedure results in a greater number of hybrids than the H_2O rinse alone. Second, the number of hybrids in the A_nT_{15} films increases with increasing length of the d(A) block. This is expected, as longer d(A) blocks increase the potential for a larger separation between the sensing d(T) blocks and thus greater accessibility for the target strands.

In the case of the $A_{15}T_{15}$, we expect that in its as-deposited state this film has a rather high degree of intramolecular hybridization. However, any molecules that remain after the post-deposition 1 min rinsing with pure water would have to be either at least partially attached to the surface via the d(A) block or hybridized to a surface-bound molecule. Previous work examining the stability of surface-bound DNA hybrids has shown them to be quite unstable and readily broken apart and replaced by a fully complimentary, non-surface-bound target molecule [12], although it should be noted that those hybrids were not formed first in solution. In diblock-oligonucleotide system used here, the lowest energy state

will be with the d(A) portion of the molecule fully adsorbed to the gold substrate and the d(T) portion fully hybridized. Thus, it is expected that the introduction of the A_{15} targets would break apart most of the inter or intra-molecular hybrids in the $A_{15}T_{15}$ layer.

The change in adenine content made clear by HRXPS was also observed with IRRAS. The spectra from $A_{15}T_{15}$/Au before and after hybridization are shown in Figure 5, in which the intensity of the adenine-specific peak at 1650 cm^{-1} increases relative to the thymine-specific peak at 1707 cm^{-1} from the unhybridized films to those rinsed with H_2O prior to hybridization. This peak increases further in the film treated with the H_2O-NaOH rinsing procedure.

The NEXAFS data for the hybrid brushes are presented in Figure 6. The N K-edge spectra collected at 55° (left panels) showed an increase in the intensity of the adenine-assigned resonance at 399.4 eV relative to the thymine contribution at 401.6 eV after hybridization compared to the analogous spectra for the unhybridized films (Figure 3, left), supporting the results of the other techniques. Furthermore, the spectra exhibit an increase in the intensity of the adenine-assigned resonance relative to the thymine contribution for all films rinsed with alternating H_2O and NaOH over those rinsed with just H_2O prior to hybridization, an effect which is especially pronounced for A_5T_{15}/Au. This indicates a higher

Figure 5 IRRAS spectra of the $A_{15}T_{15}$ film in an unhybridized state (lower spectrum), after rinsing with only H_2O and hybridizing (middle spectrum), and after rinsing with H_2O-NaOH and hybridizing (upper spectrum). The adenine (A) portion can be seen to increase relative to the thymine (T) portion from the unhybridized to the H_2O-rinsed, and from the H_2O-rinsed to the H_2O and NaOH-rinsed film.

adenine content in the NaOH-treated layers, in agreement with both the HRXPS (Figure 4) and IRRAS (Figure 5) results. The information gathered from the 90˚–20˚ difference spectra reveals significant changes in orientation in these films relative to their unhybridized counterparts, especially in the case of A_5T_{15}/Au (Figure 3). The A_5T_{15}/Au sample, which unhybridized had shown a positive adenine difference peak and nearly no thymine difference peak, now clearly displays negative peaks for both nucleobase types. This indicates that the predominant orientation of both the d(A) and d(T) blocks present in this film is perpendicular to the surface. This agrees qualitatively with the idealized model (Scheme 1), with the A_5 block of the A_5T_{15} probes adhering parallel to the substrate and the T_{15} block protruding from the surface and hybridizing with the A_{15} target. In spite of the limited extent of hybridization (see above), the spectral contribution of the A_{15} targets is clearly higher than that of the A_5 anchors. This is related

to the greater number of adenine nucleotides in the A_{15} targets versus the A_5T_{15} molecules (as far as one compares the individual species) as well as to a stronger attenuation of the PEY signal from the A_5 anchors as compared to the perpendicularly-oriented A_{15} probes (this effect is smaller as compared to the photoelectrons but still applicable [43]). Interestingly, the difference peaks increase in intensity for the film rinsed with the H_2O-NaOH rinsing procedure, indicating a slightly improved orientation of the hybrids in this sample. This means that a rinse including NaOH is more efficient for the disruption of inter- or intramolecular hybrids in the probe film before the hybridization, making the T_{15} strands of assembled A_5T_{15} more easily accessible to the target molecules.

Hybridization of the $A_{10}T_{15}$/Au film also causes a previously positive adenine-assigned difference peak (Figure 3) to become negative, indicating a change in the orientation of the majority of the adenine strands from parallel to perpendicular to the surface after hybridization. This behavior also agrees qualitatively with the idealized model of the $A_{10}T_{15}$/Au:A_{15} hybrids (Scheme 1), assuming that the ideal L-shape is significantly distorted. Also in this case, the spectral contribution of the perpendicularly-oriented A_{15} probes is clearly higher than that of the parallel A_{10} anchors. This is similar to what was observed for the A_5T_{15}/Au:A_{15} film, and can likely be explained by the same reasoning. However, in contrast to A_5T_{15}/Au:A_{15}, there is no significant change in either the orientation or intensity of these peaks between the H_2O-rinsed samples and those subjected to the H_2O-NaOH rinsing procedure. As previously mentioned, this may be due to the relative instability of hybrids with few base pairs [26,40]. The few intermolecular hybrids that were present in the film after rinsing but before hybridization may have been unstable enough to be replaced by a more energetically stable $A_{10}T_{15}$:A_{15} hybrid, regardless of whether the brush was exposed to NaOH or only H_2O.

Both of the hybridized $A_{15}T_{15}$/Au samples show negative adenine- and thymine-assigned difference peaks, as was the case in the unhybridized layer. However, the dichroism becomes more pronounced after hybridization, which is especially obvious for the adenine-assigned difference peak. This increase in the dichroism can be associated with the contribution of the perpendicularly-oriented A_{15} targets, which have a particularly high spectral weight due to the high degree of hybridization (see above). The ideal L-shape model (Scheme 1) is likely also applicable in this case, at least qualitatively (under the assumption of distortion), given the high degree of hybridization. However, the comparably large spacing between the individual hybrids should diminish the orientational order, as usually occurs for loosely packed molecular films. This effect should be less pronounced
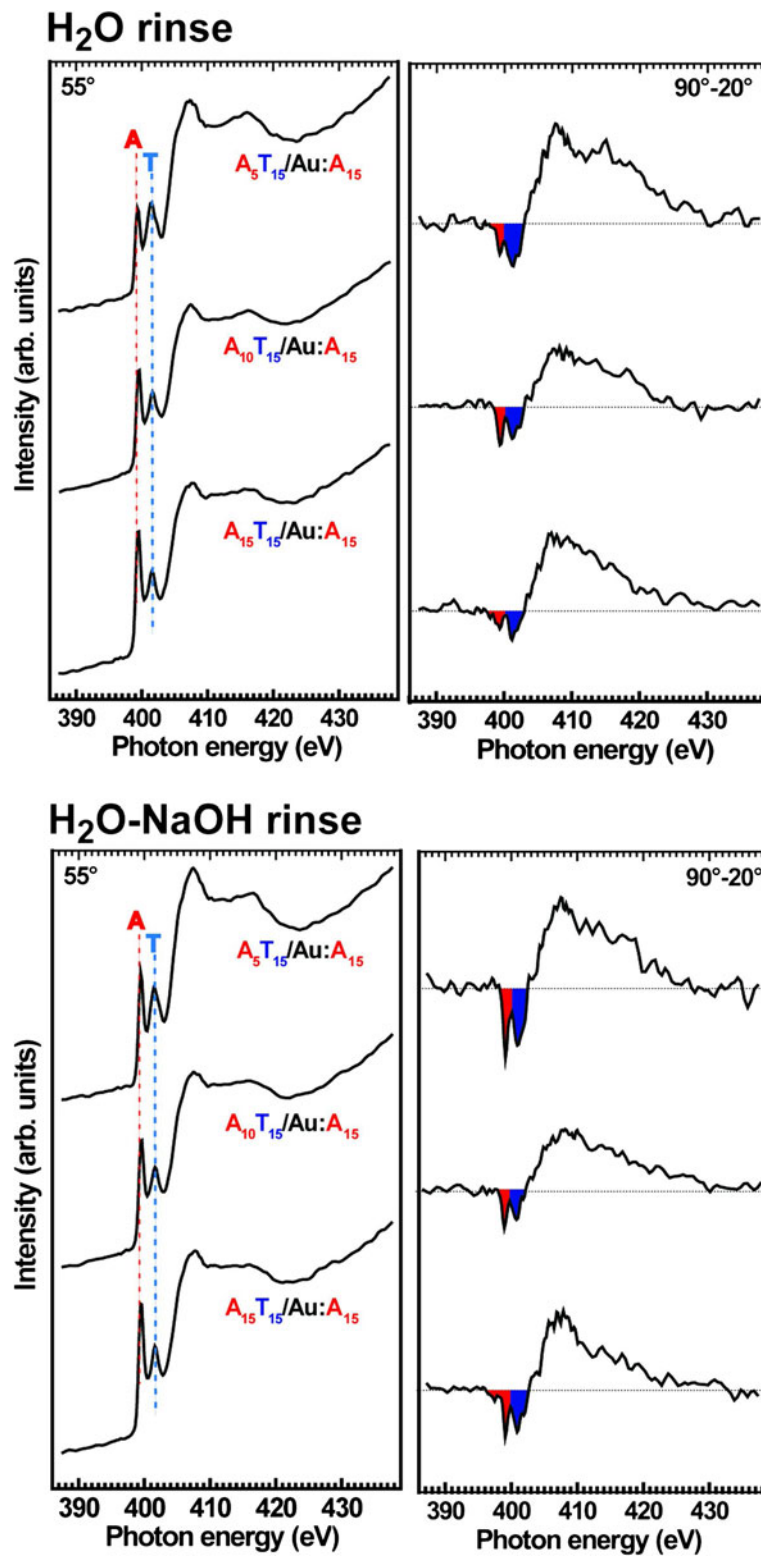
Figure 6 (See legend on next page.)

(See figure on previous page.)
Figure 6 N K-edge NEXAFS spectra of the A_nT_{15} brushes after rinsing with only H_2O (upper panels) or with H_2O-NaOH (lower panels) followed by hybridization with an A_{15} target. Left panels: Spectra acquired at an X-ray incidence angle of 55°. The positions of the most pronounced, π*-like absorption resonances of thymine (T) and adenine (A) are marked by the thin vertical blue (T) or red (A) dotted lines. Right panels: Difference of the spectra acquired at X-ray incidence angles of 90° and 20°. Adenine and thymine contributions are indicated by the red or blue fill (respectively), with an upward or downward direction indicating a preferentially horizontal or vertical orientation (respectively) of the DNA strand relative to the surface. Horizontal dashed lines correspond to zero for the individual difference spectra.

in $A_{10}T_{15}/Au:A_{15}$ and least pronounced in $A_5T_{15}/Au:A_{15}$. Indeed, the latter film exhibits the highest extent of dichroism as compared to the two others, especially in the case of the film rinsed with alternating H_2O and NaOH.

Returning to $A_{15}T_{15}/Au:A_{15}$ and comparing the difference spectra for the cases of H_2O and H_2O-NaOH rinsing procedures, we can state that the addition of NaOH only slightly improves the orientational order in the hybrid films. Presumably, as mentioned above, the orientational order is limited by the low packing density and the improvement is solely related to the higher extent of hybridization in the case of the film treated with the H_2O-NaOH rinsing procedure.

Conclusions

We have examined a series of adenine/thymine diblock-oligonucleotide films and their hybrid brushes using a combination of HRXPS, IRRAS, and NEXAFS spectroscopy to monitor sample composition as well as molecular orientation and ordering. As probe films, we used adenine-thymine diblock oligonucleotides composed of either 5, 10, or 15 adenine nucleotides [d(A)] connected to 15 thymine nucleotides [d(T)]. The quality and composition of these films was confirmed by the HRXPS, IRRAS, and NEXAFS composition data, while the binding function of the adenine block was confirmed by the HRXPS data. It was found that the orientational order in these films differed significantly from the ideal L-shape model, in which the binding d(A) block is oriented strictly parallel to the substrate while the d(T) portion of the molecule extends away and can be used to form hybrids with a complimentary target. In reality, the situation appeared to be more complex, a fact which was explained by inter- and intramolecular hybridization within the monomolecular assemblies. Deviations from the ideal model were observed in all probe films of the present study but became more pronounced with increasing length of the d(A) binding block and subsequently increased potential for stable inter- and intramolecular hybridization.

In spite of the complex molecular arrangements, all probe films performed well upon hybridization with the A_{15} target, exhibiting the expected correlation between the lateral density (i.e. accessibility) of the probe T_{15} strands and the extent of hybridization. Whereas this extent was relatively low for the most densely packed A_5T_{15} films, it was found to increase the $A_{10}T_{15}$ samples, and was highest in the most loosely packed $A_{15}T_{15}$ monolayers. Furthermore, it was observed that the probe films rinsed with alternating H_2O and NaOH exhibited higher hybridization efficiency than the films rinsed with H_2O only. This confirms the ability of NaOH to reduce the number of surface-bound inter- and intramolecular hybrids, favoring more efficient hybridization.

The NEXAFS data for the hybrid $A_nT_{15}/Au:A_{15}$ brushes do not contradict the ideal L-shape model but do not unequivocally support it. One can only say for sure that the $T_{15}:A_{15}$ hybrids have the expected predominantly upright orientation, with the highest orientational order present in the most densely packed $A_5T_{15}/Au:A_{15}$ brush. It is, however, difficult if not impossible to monitor the orientation of the binding A_n blocks since their contributions to the spectra are masked by those of the of the A_{15} targets. However, a parallel-to-the-substrate orientation of the binding blocks can be assumed to be most likely in view of the extensive disruption of the inter- and intramolecular hybrids in the probe film upon rinsing and subsequent hybridization.

These results are a good illustration of the strength of spectroscopic analysis in its specific application to biological systems, demonstrating that the use of different techniques to observe multiple facets of the system can often reveal unexpected effects. In some cases, such effects may prove to be key factors in understanding biological properties and processes on surfaces and interfaces at the molecular level.

Authors' contributions
CH and MZ conceived of and designed the study, CH fabricated the samples and performed the IRRAS measurements and analysis, MZ and HH carried out the NEXAFS and HRXPS measurements and analysis. CH and MZ wrote the manuscript. All authors read and approved the final manuscript

Author details
[1]Institute of Toxicology and Genetics, Karlsruhe Institute of Technology, Hermann-von-Helmholtz-Platz 1, 76344, Eggenstein-Leopoldshafen, Germany. [2]Applied Physical Chemistry, University of Heidelberg, Im Neuenheimer Feld 253, 69120, Heidelberg, Germany. [3]Present address: School of Engineering and Applied Sciences, Harvard University, 29 Oxford St, Cambridge, MA 02138, USA. [4]Present address: International Center for Materials Nanoarchitectonics, Institute for Materials Science, Namiki 1-1, Tsukuba, Ibaraki, Japan.

References
1. Castner DG, Ratner BD: **Biomedical surface science: Foundations to frontiers.** *Surf Sci* 2002, **500**:28–60.
2. Höök F, Kasemo B, Grunze M, Zauscher S: **Quantitative biological surface science: Challenges and recent advances.** *ACS Nano* 2008, **12**:2428–2436.
3. Kasemo B: **Biological surface science.** *Surf Sci* 2002, **500**:656–667.
4. Cosnier S, Mailley P: **Recent advances in DNA sensors.** *Analyst* 2008, **133**:984–991.
5. Hsiao SC, Shum BJ, Onoe H, Douglas ES, Gartner ZJ, Mathies RA, Bertozzi CR, Francis MB: **Direct cell surface modification with DNA for the capture of primary cells and the investigation of myotube formation on defined patterns.** *Langmuir* 2009, **25**:6985–6991.
6. Mirkin CA, Letsinger RL, Mucic RC, Storhoff JJ: **A DNA-based method for rationally assembling nanoparticles into macroscopic materials.** *Nature* 1996, **382**:607–609.
7. Storhoff JJ, Mirkin CA: **What controls the optical properties of DNA-linked gold nanoparticle assemblies?** *Chem Rev* 1999, **99**:1849–1862.
8. Adleman LM: **Molecular computation of solutions to combinatorial problems.** *Science* 1994, **266**:1021–1024.
9. Liu Q, Wang L, Frutos AG, Condon AE, Corn RM, Smith LM: **DNA computing on surfaces.** *Nature* 2000, **403**:175–179.
10. Bally M, Halter M, Vörös J, Grandin HM: **Optical microarray biosensing techniques.** *Surf Int Anal* 2006, **38**:1442–1458.
11. Schreiner SM, Shudy DF, Hatch AL, Opdahl A, Whitman LJ, Petrovykh DY: **Controlled and Efficient Hybridization Achieved with DNA Probes Immobilized Solely through Preferential DNA-Substrate Interactions.** *Anal Chem* 2010, **2010**(82):2803–2810.
12. Schreiner S, Hatch A, Shudy D, Howell C, Zhao J, Koelsch P, Zharnikov M, Petrovykh D, Opdahl A: **Impact of DNA–Surface Interactions on the Stability of DNA Hybrids.** *Anal Chem* 2011, **83**:4288–4295.
13. Petrovykh DY, Kimura-Suda H, Whitman LJ, Tarlov MJ: **Quantitative analysis and characterization of DNA immobilized on gold.** *J Am Chem Soc* 2003, **125**:5219–5226.
14. Petrovykh DY, Kimura-Suda H, Tarlov MJ, Whitman LJ: **Quantitative characterization of DNA films by X-ray photoelectron spectroscopy.** *Langmuir* 2004, **20**:429–440.
15. Petrovykh DY, Perez-Dieste V, Opdahl A, Kimura-Suda H, Sullivan JM, Tarlov MJ, Himpsel FJ, Whitman L: **Nucleobase orientation and ordering in films of single-stranded DNA on gold.** *J Am Chem Soc* 2006, **128**:2–3.
16. Lee CY, Gong P, Harbers GM, Grainger DW, Castner DG, Gamble LJ: **Surface coverage and structure of mixed DNA/alkylthiol monolayers on gold: characterization by XPS, NEXAFS, and fluorescence intensity measurements.** *Anal Chem* 2006, **78**:3316–3325.
17. Ballav N, Koelsch P, Zharnikov M: **Orientation and Ordering in Monomolecular Films of Sulfur-Modified Homo-oligonucleotides on Gold.** *J Phys Chem C* 2009, **113**:18312–18320.
18. Howell C, Zhao J, Koelsch P, Zharnikov M: **Hybridization in ssDNA films—a multi-technique spectroscopy study.** *Phys Chem Chem Phys* 2011, **13**:15512–15522.
19. Lee CY, Canavan HE, Gamble LJ, Castner DG: **Evidence of impurities in thiolated single-stranded DNA oligomers and their effect on DNA self-assembly on gold.** *Langmuir* 2005, **21**:5134–5141.
20. Lee C-Y, Gamble LJ, Grainger DW, Castner DG: **Mixed DNA/Oligoethylene glycol functionalized gold surfaces improve DNA hybridization in complex media.** *Biointerphases* 2006, **1**:83–92.
21. Lee CY, Nguyen PCT, Grainger DW, Gamble LJ, Castner DG: **Structure and DNA hybridization properties of mixed nucleic acid/maleimide-ethylene glycol monolayers.** *Anal Chem* 2007, **79**:4390–4400.
22. Stokes GY, Gibbs-Davis JM, Boman FC, Stepp BR, Condie AG, Nguyen ST, Geiger FM: **Making "Sense" of DNA.** *J Am Chem Soc* 2007, **129**:7492–7493.
23. Howell C, Jeyachandran YL, Koelsch P, Zharnikov M: **Orientation and Ordering in Sequence-and Length-Mismatched Surface-Bound DNA Hybrids.** *J Phys Chem C* 2012, **116**:11133–11140.
24. Opdahl A, Petrovykh DY, Kimura-Suda H, Tarlov MJ, Whitman L: **Controlled and Efficient Hybridization Achieved with DNA Probes Immobilized Solely through Preferential DNA-Substrate Interactions.** *J Proc Natl Acad Sci USA* 2007, **104**:9–14.
25. Saprigin AV, Thomas CW, Dulcey CS, Patterson CH, Spector MS: **Spectroscopic quantification of covalently immobilized oligonucleotides.** *Surf Int Anal* 2005, **37**:24–32.
26. Howell C, Hamoudi H, Koelsch P, Zharnikov M: **Orientation changes in surface-bound hybridized DNA undergoing preparation for ex situ spectroscopic measurements.** *Chem Phys Lett* 2011, **513**:267–270.
27. Zharnikov M, Grunze M: **Modification of thiol-derived self-assembling monolayers by electron and x-ray irradiation: Scientific and lithographic aspects.** *J Vac Sci Technol B* 2002, **20**:1793–1807.
28. Heister K, Zharnikov M, Grunze M, Johansson LSO, Ulman A: **Characterization of X-ray induced damage in alkanethiolate monolayers by high-resolution photoelectron spectroscopy.** *Langmuir* 2001, **17**:8–11.
29. Wirde M, Gelius U, Dunbar T, Allara DL: **Modification of self-assembled monolayers of alkanethiols on gold by ionizing radiation.** *Nucl Instrum Methods Phys Res B* 1997, **131**:245–251.
30. Jäger B, Schürmann H, Müller HU, Himmel HJ, Neumann M, Grunze M, Wöll C: **X-ray and low energy electron induced damage in alkanethiolate monolayers on Au-substrates.** *Z Phys Chem* 1997, **202**:263–272.
31. *Surface chemical analysis – X-ray photoelectron spectrometers – Calibration of the energy scales.* ISO; 2001:15472.
32. Thome J, Himmelhaus M, Zharnikov M, Grunze M: **Increased lateral density in alkanethiolate films on gold by mercury adsorption.** *Langmuir* 1998, **14**:7435–7449.
33. Lamont CLA, Wilkes J: **Attenuation length of electrons in self-assembled monolayers of n-alkanethiols on gold.** *Langmuir* 1999, **15**:2037–2042.
34. Stöhr J: *NEXAFS Spectroscopy, Springer Series in Surface Science 25.* Berlin: Springer; 1992.
35. Batson PE: **Carbon 1s near-edge-absorption fine structure in graphite.** *Phys Rev B: Condens Matter* 1993, **48**:2608–2610.
36. Kimura-Suda H, Petrovykh DY, Tarlov MJ, Whitman LJ: **Base-dependent competitive adsorption of single-stranded DNA on gold.** *J Am Chem Soc* 2003, **125**:9014–9015.
37. Zubavichus Y, Shaporenko A, Korolkov V, Grunze M, Zharnikov M: **X-ray Absorption Spectroscopy of the Nucleotide Bases at the Carbon, Nitrogen, and Oxygen K-Edges.** *J Phys Chem B* 2008, **112**:13711–13716.
38. Samuel NT, Lee CY, Gamble LJ, Fischer DA, Castner DG: **NEXAFS characterization of DNA components and molecular-orientation of surface-bound DNA oligomers.** *J Electron Spectrosc Relat Phenom* 2006, **152**:134–142.
39. Peterson AW, Wolf LK, Georgiadis RM: **Hybridization of mismatched or partially matched DNA at surfaces.** *J Am Chem Soc* 2002, **124**:14601–14607.
40. Hagan MF, Chakraborty AK: **Hybridization dynamics of surface immobilized DNA.** *J Chem Phys* 2004, **10**:4958–4968.
41. Shamsi MH, Kraatz HB: **The effects of oligonucleotide overhangs on the surface hybridization in DNA films: an impedance study.** *Analyst* 2011, **136**:3107–3112.
42. Lane MJ, Paner T, Kashin I, Faldasz BD, Li B, Gallo FJ, Benight AS: **The thermodynamic advantage of DNA oligonucleotide 'stacking hybridization'reactions: energetics of a DNA nick.** *Nucleic Acids Res* 1997, **25**:611–616.
43. Zharnikov M, Frey S, Heister K, Grunze M: **An extension of the mean free path approach to X-ray absorption spectroscopy.** *J Electron Spectrosc Relat Phenom* 2002, **124**:15–24.